Silicon nanowire detectors showing phototransistive gain

Arthur Zhang,[1,a)] Sifang You,[2] Cesare Soci,[1] Yisi Liu,[3] Deli Wang,[1] and Yu-Hwa Lo[1]
[1]*Department of Electrical and Computer Engineering, Jacobs School of Engineering, University of California-San Diego, La Jolla, California 92093, USA*
[2]*Department of Physics, University of California-San Diego, La Jolla, California 92093, USA*
[3]*Agiltron, Inc., 15 Cabot Road, Woburn, Massachusetts 01801, USA*

(Received 19 May 2008; accepted 8 September 2008; published online 25 September 2008)

Nanowire photodetectors are shown to function as phototransistors with high sensitivity. Due to small lateral dimensions, a nanowire detector can have low dark current while showing large phototransistive gain. Planar and vertical silicon nanowire photodetectors fabricated in a top-down approach using an etching process show a phototransistive gain above 35 000 at low light intensities. Simulations show that incident light can be waveguided into vertical nanowires resulting in up to 40 times greater external quantum efficiency above their physical fill factor. Vertical silicon nanowire phototransistors formed by etching are attractive for low light level detection and for integration with silicon electronics. © *2008 American Institute of Physics*.
[DOI: 10.1063/1.2990639]

Silicon (Si) photodetectors have many applications including optical interconnects and image sensor arrays. Due to the small lateral dimensions and the large surface-to-volume ratio of Si nanowires (NWs), the large number of states at a Si surface can trap carriers at the surface equivalent to a gate bias, resulting in phototransistive behavior that leads to high sensitivity. This unique property of Si NWs makes these devices attractive for photodetection from ultraviolet (UV) to the near infrared. Previously, Si NW photodetectors were demonstrated in both chemical vapor deposition grown[1–3] and planar-etched devices,[4–6] but measurement of the gain was not reported. Although Si NWs can easily be grown, precise NW positioning has always been an obstacle and has limited their application for arrayed devices. To address these issues, etched planar and vertical Si NW photodetectors have been fabricated and characterized, and their gain evaluated. Etching of NW devices allows for specific placement of wires to easily form arrays and integrate into complementary metal-oxide-semiconductor circuits.

Any planar NW device, fabricated by either top-down or bottom-up techniques, will suffer from a low physical fill factor (FF), limiting the net detection efficiency. Physical FF is defined as the percentage of photoactive area inside the total pixel area. However, for vertical NW devices, we have shown through simulations that the seemingly low physical FF is significantly improved due to the refractive index difference between vertical wires and their surroundings. This causes incident light to be waveguided into the wires, increasing their effective coupling efficiency well above what would be expected from the physical FF.

Planarly etched Si NW devices were created from a *p*-type ⟨100⟩ silicon-on-insulator (SOI) wafer with doping $\sim 10^{15}$ cm^3. NWs were created by using a photolithographically patterned oxide mask. By using buffered oxide etch to isotropically etch the mask, features much smaller than the lithographic pattern were produced. The exposed Si was then anisotropically etched using potassium hydroxide. The wires were then passivated with a thin layer of dry thermal oxide grown at 1000 °C. To form electrical contacts, nickel (Ni) was deposited and annealed to form Ni silicide, and a final metallization of aluminum (Al) was deposited. A scanning electron microscope (SEM) image of a multi-NW device with wires 250 nm in width and thickness and 8 μm in length is shown in Fig. 1(a).

Vertical NWs were fabricated from a *p*-type Si wafer, with doping $\sim 10^{15}$ cm^3, through dry etching. Electron beam lithography was used to pattern arrays of nanoscale dots onto poly(methyl methacrylate) photoresist (MicroChem). Then Ni was deposited and lifted off, transferring the pattern to a Ni mask. Subsequently, an inductively coupled plasma/reactive ion etch process at room temperature was used to anisotropically etch NWs from the Ni disks. This created vertical arrays of NWs shown in Fig. 1(b) with a diameter of 200 nm and length of 2.7 μm. An Al contact was sputtered on the backside of the substrate. The wire array was then filled with a UV transparent polymer and the wire tips exposed by dry etching the polymer. Filling the space between wires with polymer provides structural support for a transparent top contact while allowing visible and UV light to reach the device. A transparent indium-tin-oxide layer was deposited to make contact with the Ni disks on top of the Si NWs. A final metal layer was evaporated and lifted off to form contact pads away from the photosensitive area.

The optical response of fabricated devices was characterized in the dark and under UV illumination using a mercury vapor lamp with a band-pass filter centered at 390 nm (± 50 nm). The UV illumination intensity was varied using neutral density filters. Devices were directly probed and measured using an Agilent 4155B parameter analyzer.

dc measurements of a planar 10 NW array device under dark and varying illumination are shown in Fig. 2 and are representative of both planar and vertical structures. The structures created show a one-sided Schottky contact most likely due to asymmetries in metal deposition during fabrication. Measurements taken by forward biasing the junction are seen in Fig. 2(a). The device shows very little current and no photoresponse when the junction is reverse biased. The gain G of this detector is defined as $G=I/eF$ where I is the photocurrent, e is the elementary charge, and F is the photon

a)Electronic mail: ayzhang@uscd.edu.

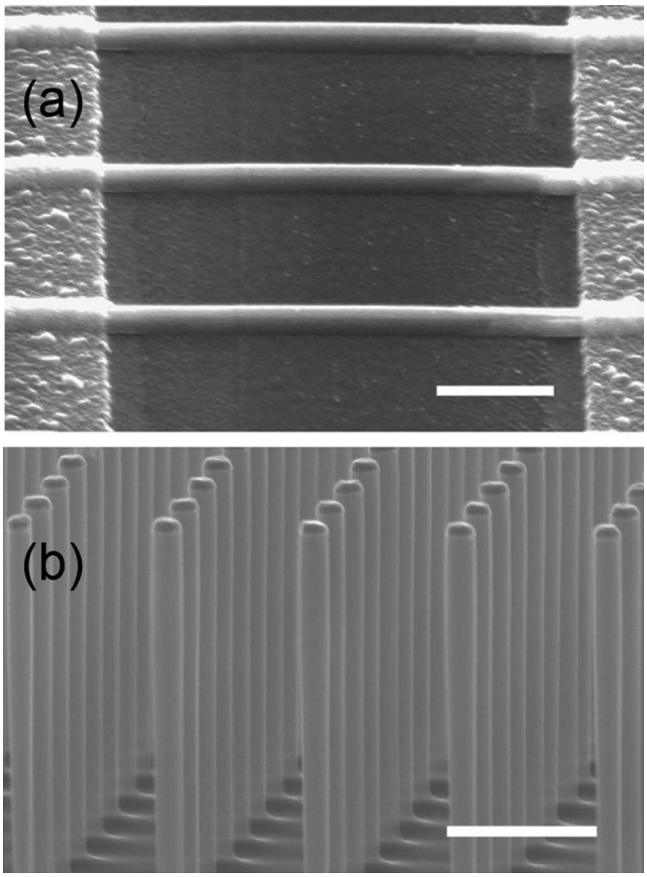

FIG. 1. (a) SEM of planar-etched multi-NW Si photodetector fabricated from a SOI wafer. The wires are 250 nm in diameter and 8 μm in length. The device sits on the buried oxide and is contacted using Al above Ni silicide. Scale bar is 2 μm. (b) SEM of vertical-etched Si NW array device. The wires are 200 nm in diameter and 2.7 μm in length with 1 μm spacing. Scale bar is 1 μm.

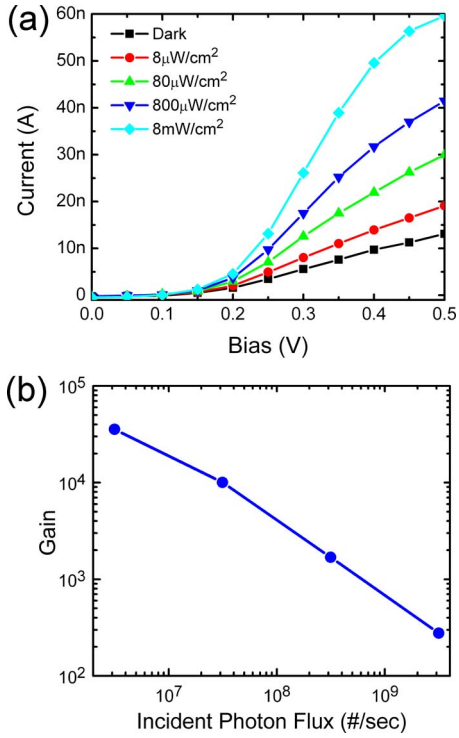

FIG. 2. (Color online) (a) *IV* characteristics of planar 10 NW device in dark and under various illumination intensities. Each wire is 250 nm in diameter and 8 μm in length. (b) Gain vs estimated photon flux incident on the exposed NW area for this NW device biased at 0.5 V.

flux per second. The gain versus the estimated photon flux of this device is shown in Fig. 2(b). The photon flux was estimated for an exposed area of 10 NWs, each having dimensions of 250 nm in width and 8 μm in length, assuming that 33% of the light incident on the exposed area was absorbed (this number was derived from 45% surface reflection and 60% absorption in Si for 230 nm wire thickness at $\lambda = 390$ nm). Figure 2(b) shows a large gain saturation at high light intensities, but a large gain of 35 000 is achieved at the lowest available light intensity, suggesting that the device holds promise at even lower light intensities as responsivity further increases toward the single photon limit.

The gain in these NW devices arises from the phototransistive effect of trapped carriers at the surface acting as an optically modulated gate.[7] The increase in carrier lifetime has been found in other NW devices such as those of zinc oxide (ZnO),[7] where the geometry of the NW enhances the lifetime through spatial charge separation. The phototransistive effect was also previously demonstrated in quantum dot phototransistors where the quantum dots act as the carrier trap, creating an optically modulated gate leading to a high gain and allowing detection down to the single photon level.[8] In our Si NW device under dark conditions, the small number of free carriers in the body of the NW (holes in this case), resulting from the small volume of the NW, is trapped at the much larger number of surface states. From simple calculations using Gauss's law and electrostatics for a uniformly charged cylinder, it can be shown that the number of surface states required to completely deplete the NW with 10^{15} cm^3 doping is 10^{10} cm^{-2}. With our oxidation conditions, the surface state density is expected to be on the order of 10^{12} cm^{-2} eV^{-1},[9] which is two orders of magnitude larger than that required to deplete the NWs in our geometry; hence an effective gate bias and a built-in lateral field exist between trapped carriers (holes) and ionized impurities (acceptors) due to the complete depletion of the NW. When an electron/hole pair is generated by photon absorption, the electron is swept to the surface of the NW due to the lateral field and the small radius of the NW where it recombines with a trapped hole. However, the photogenerated hole is confined to the center of the NW by the lateral field and contributes to the current over a longer time until it is finally trapped at the surface. Phototransistive gain seen in our experiments is achieved by the large difference between the long lifetime of holes and the transit time and can also be expressed as $G = \tau_l / \tau_t$ where τ_l is the hole lifetime and τ_t is the hole transit time.

Although the small size of the NWs is responsible for the unique optoelectronic properties leading to large gain, it also limits these devices with an intrinsically low physical FF. The photosensitive NW area is only a small fraction of the light-exposed area, causing a very small physical FF and thus low external quantum efficiency. However, this problem can be alleviated with vertical NW devices, where the refractive index difference between the high index Si NW and low index surrounding material can cause a waveguiding effect that presents a large numerical aperture that funnels incoming light. The effective physical FF is much larger, improving the external quantum efficiency. The enhancement of optical coupling was verified in simulations using COMSOL

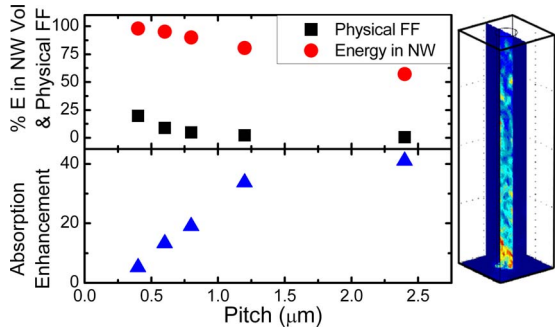

FIG. 3. (Color online) Upper plot: simulation results using COMSOL MULTIPHYSICS of vertical NW structure. The graph shows the electric field energy inside two-dimensional NW arrays with varying pitch. The simulation demonstrates that the presence of the higher index NW enhances the energy inside the wires above the physical FF. Lower plot: absorption enhancement of NWs (ratio of the percentage of total energy absorbed in the NW to physical FF) with increasing pitch. As pitch increases, the waveguiding effect becomes more pronounced. Inset: a visual representation of the energy confinement in the simulation results.

MULTIPHYSICS software models. An infinite array of 200 nm diameter and 2 μm long NWs was used in the simulations with the following boundary conditions: perfectly reflecting bottom surface and periodic wire structure. Incident UV light ($\lambda=350$ nm) was set normal to the top surface. A complex refractive index ($\tilde{n}=5.43+3.15i$) corresponding to the input wavelength was used for Si, while an index of $n=1.6$ for a generic UV transparent polymer was used in the surrounding material. Figure 3 shows the results of the simulations with varying pitch; the right inset of Fig. 3 shows a visual representation of the energy distribution in one of the simulated structures having a 0.6 μm pitch. The results in the upper plot of Fig. 3 show that the percentage of photon energy within the NW volume is significantly larger than the physical FF, especially at larger pitch. To verify that the chosen geometry and boundary conditions did not have an effect on the energy distribution calculated inside the wires, we have also repeated the simulations assuming an index of 1.6 for the NWs (i.e., matching the polymer index so that no waveguiding effect is expected). The results of these control experiments show no enhancement above the physical FF and thus confirm that the enhancement in quantum efficiency is caused by the light funneling effect into the NW array. The absorption enhancement due to the effect of waveguiding is quantified in the lower plot of Fig. 3 as the ratio of the percentage of energy absorbed in the NW volume above the physical FF. As expected, the enhancement approaches unity with decreasing pitch and increases substantially with increasing pitch. This demonstrates the potential for vertical NW array devices to overcome the barrier of low physical FF.

To summarize, etched planar and vertical Si NWs that function as phototransistors have been fabricated and characterized under UV illumination. Gain exceeding 35 000 is observed in these devices at low light intensities, demonstrating their potential for low light detection. Using a top-down approach to form lithographically defined, etched NWs, it is possible to overcome the limitations caused by nonuniformity, random placement, and low physical FF. While the low physical FF reduces the contribution of dark current, simulations demonstrate that in the case of vertical NWs, strong waveguiding effects cause a large fraction of the photon energy to be funneled into the NWs, increasing the effective physical FF for light gathering.

This study was partially supported by the Department of Homeland Security under SBIR Contract No. HSHQDC-07-C-00045, the U.S. Department of Energy under SBIR Contract No. DE-FG02-07ER86297, the Office of Naval Research (ONR Grant No. 050101-071231), a National Science Foundation Graduate Research Fellowship, and Sharp Laboratories of America.

[1] Y. Ahn, J. Dunning, and J. Park, Nano Lett. **5**, 1367 (2005).
[2] K. H. Kim, K. Keem, D. Y. Jeong, B. Min, K. Cho, H. Kim, B. M. Moon, T. Noh, J. Park, and M. Suh, Jpn. J. Appl. Phys., Part 1 **45**, 4265 (2006).
[3] P. Servati, A. Colli, S. Hofmann, Y. Q. Fu, P. Beecher, Z. A. K. Durrani, A. C. Ferrari, A. J. Flewitt, J. Robertson, and W. I. Milne, Physica E (Amsterdam) **38**, 64 (2007).
[4] H. G. Choi, Y. S. Choi, Y. C. Jo, and H. Kim, Digest of Papers 2003 International Microprocesses and Nanotechnology Conference, 2003 (unpublished), pp. 296–297.
[5] H. Fujii, S. Kanemaru, T. Matsukawa, H. Hiroshima, H. Yokoyama, and J. Itoh, Jpn. J. Appl. Phys., Part 1 **37**, 7182 (1998).
[6] J. H. Park, S. H. Seo, I. S. Wang, H. J. Yoon, J. K. Shin, P. Choi, Y. C. Jo, and H. Kim, Jpn. J. Appl. Phys., Part 1 **43**, 2050 (2004).
[7] C. Soci, A. Zhang, B. Xiang, S. A. Dayeh, D. P. R. Aplin, J. Park, X. Y. Bao, Y. H. Lo, and D. Wang, Nano Lett. **7**, 1003 (2007).
[8] E. J. Gansen, M. A. Rowe, M. B. Greene, D. Rosenberg, T. E. Harvey, M. Y. Su, R. H. Hadfield, S. W. Nam, and R. P. Mirin, Nat. Photonics **1**, 585 (2007).
[9] R. R. Razouk and B. E. Deal, J. Electrochem. Soc. **126**, 1573 (1979).